Determination and Verification of the Forchheimer Coefficients for Ceramic Foam Filters Using COMSOL CFD Modelling

Mark W. Kennedy*[1], Kexu Zhang[1], Jon Arne Bakken[1] and Ragnhild E. Aune[1,2]
[1]Dept. of Mat. Sci. and Eng., Norwegian University of Science and Tech. (NTNU), Norway
[2]Dept. of Materials Science and Engineering, Royal Institute of Technology (KTH), Sweden
*Communicating author: mark.kennedy@material.ntnu.no, mark.kennedy@metallurgy.no

Abstract: Experiments have been conducted with water at velocities from ~0.015-0.77 m/s to determine the permeability of 50 mm thick commercially available 30, 40, 50 and 80 Pores Per Inch (PPI) alumina Ceramic Foam Filters (CFF) used for liquid metal filtration.

Measurements were made using two different experimental setups, i.e. the 49 mm diameter 'straight through' and 101 mm diameter 'expanding flow field' designs. Difficulties were encountered in regards to sealing the 'straight through' design to prevent flow bypassing, as well as defining an effective diameter for the 'expanding flow field' design for use with the Forchheimer equation.

2D axial symmetric CFD modelling, using COMSOL® 4.2a, has been performed to show that the two experimental designs delivered equivalent permeability data. Based on the obtained outcome from the modelling it has been shown that COMSOL can give results with <7% error by including the Forchheimer second order term in the model for the porous media. This was also the case for flows at high pore Reynolds numbers.

Keywords: Ceramic Foam Filter, CFF, Permeability, Forchheimer, CFD

1. Introduction

Inclusions in liquid aluminium can have serious detrimental effects on the properties of the metal as well as on the performance of products produced from such metal [1-6]. Typical particle sizes cover a large range from 0.1 to 50 μm [7]. Ceramic Foam Filters (CFFs) have since the 1990's been used to filter inclusions from more than 50% of the aluminium produced world wide [4]. A typical CFF with 30 Pores Per Inch (PPI) is presented in Figure 1. CFFs are normally capable of removing particulate inclusions larger then 20 μm with an efficiency exceeding 50% [8]. Commercial CFFs are typically 50 mm thick and operate in a filter bowl with a gravity metal head producing the driving force needed for obtaining a flow through the filter. In this regard, filter permeability is a key property which determines the required metal head to produce any given flow velocity during casting operations.

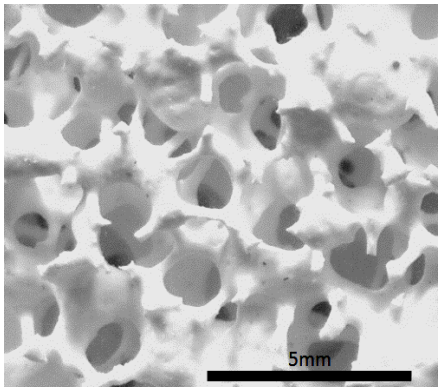

Figure 1. Image of a 30 PPI alumina CFF used for the filtration of liquid metal.

The permeability of new and clean CFFs can be conveniently determined under cold conditions using water. Water is a reasonable analogue for liquid aluminium, having the same dynamic viscosity at 20°C, as aluminium at normal casting temperatures of ~700°C. With aluminium being a light metal, the kinematic viscosity is only different by a factor of 2.4. It should, however, be pointed out that measurements made with clean water can only be directly compared with new filters. Aluminium filtration with CFFs is normally performed in deep mode, which limits the increase of pressure with time. In most cases, CFFs are changed before entering cake filtration mode, except in the case of 80 PPI filters and/or highly contaminated metal. The initial drop in

the pressure over the filter does therefore dominate the hydrodynamic behaviour of the CFFs in operation.

2. Theory

Typical superficial flow velocities during casting are low, i.e. on the order of 0.2-1.5 cm/s [7]. It is often assumed that only the viscous first order Darcy term is required to predict pressure drop at such low velocity. The transition velocity to second order inertial behaviour has, however, been shown to be as low as 1 cm/s for CFFs [9]. Due to this it is therefore necessary to know both the Darcy and the non-Darcy terms of the Forchheimer equation [10]:

$$\frac{\Delta P}{L} = \frac{\mu}{k_1} V_s + \frac{\rho}{k_2} V_s^2 \qquad (1)$$

where ΔP is the pressure drop across the CFF [Pa], L the filter thickness [m], μ the fluid viscosity (which for water at 280 K is 1.382×10^{-3} [Pa·s]), V_s the fluid superficial velocity [m/s], k_1 the first order Darcy coefficient [m^2], ρ the fluid density (which for water at 280 K is ~1000 [kg/m^3]), and k_2 the non-Darcy coefficient [m].

Equation (1) represents the sum of the viscous (first term) and the kinetic energy losses (second term). Implicit in Equation (1) is that there is flow in only the axis defined by the direction of L, e.g. the z-axis, and that a constant area or 'effective diameter' can represent the extent of the flow field. This was approximately true for the 'straight through' flow design used in the current experiments, see Figure 2 (a), but not true for the 'expanding flow field' design, see Figure 2 (b).

In order to apply Equation (1) to the 101 mm diameter experimental filters it was necessary to solve the Reynolds-Averaged Navier-Stokes (RANS) equation for flow in porous media using 2D axial symmetry. This was done to be able to account for the expansion and contraction of the flow field in the radial direction as the flow entered and exited the apparatus through the attached Plexiglas® pipes.

3. Experimental

The liquid permeability of 50 mm thick commercial CFFs with 30, 40, 50 and 80 PPI, were measured using water. Mass flows from about 0.05 to 2 kg/s of water were circulated through 46.4 mm ID smooth plastic piping, representing Reynolds numbers from ~1200-39000, and moving from laminar flow into transitional and partially turbulent pipe flow in the inlet pipe [12].

8-10 different velocities (~0.015-0.77 m/s) were used to measure the pressure drop for each filter. The 101 mm nominal diameter elements were cut from full size commercial filters using diamond bores. The 49 mm diameter filter elements were cut from the centre of the 101 mm filter elements, and thus should possess the same porosity and permeability. From the 30 to the 80 PPI CFFs the porosity varied from 89.2% to 86.5% in a roughly linear fashion [11].

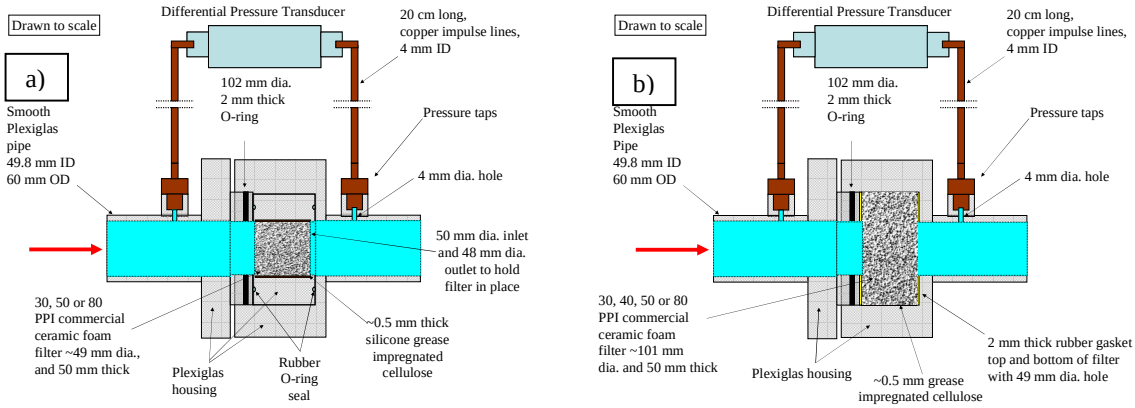

Figure 2. (a) the experimental setup used for the 50 mm thick 49 mm diameter 'straight through', and (b) the 101 mm diameter 'expanding flow field' filter experiments (both drawn approximately to scale). The flow is from left to right. For further equipment details, see reference [11].

The sealing arrangements were of critical importance in the design of the filter housings. It was necessary to prevent flow from bypassing the filters along the wall of the housing (particularly in the case of the 49 mm diameter filters), and that horizontal flow should be prevented from occurring in the case of the 101 mm filters. The various seals and gaskets used are presented in Figures 2 (a) and (b). In the final experimental setup, high viscosity silicone grease was used to smoothen the outer surface of each filter, i.e. to fill the outer-most broken or cut cells, before being wrapped in paper and pressed tightly into the holder. Upon contact with water, swelling of the cellulose fibres provided an extra seal of negligible permeability. It was necessary to seal the entire side surface of the filter, as normal O-rings would be unable to stop the flow from bypassing along the wall.

The pressure transducer used during the experiments was a DF-2 (AEP transducers, Italy) with a 0-1 bar measuring range equipped with a 4-20 mA output. The transducer was factory calibrated and certified to an error of ±0.04% over the full scale from 0-1 bar, using a 6 point calibration. The zero flow current was established to a precision of 0.001 mA (6.25 Pa), and the current during the flow measuring periods were computer data logged at 100 ms intervals by conversion to a 0-5 V signal with a resolution of 0.001V or 0.004 mA, i.e. 25 Pa resolution. The flow rate was determined from the slope of the gain-in-weight with time plot of a water receiving tank placed on a 100 kg scale having a resolution of 0.01 kg. The obtained flow rate had an error of <0.5%.

4. Use of COMSOL

In the 101 mm diameter experimental apparatus no predefined diameter existed to calculate the superficial velocity to be used with Equation (1). It was therefore necessary to iteratively solve the equation for the effective flow field diameter using a COMSOL 4.2a® 2D axially symmetric model, by adopting the procedure presented in Figure 3. This was done in order to correctly determine the Forchheimer coefficients to be used with Equation (1). For the 49 mm diameter experimental apparatus, the Forchheimer coefficients were determined directly from Equation (1) and the measured pressure gradients. The Forchheimer terms where then used with COMSOL to determine if the same pressure gradients could be calculated numerically, to ensure that no fluid leakage was occurring along the walls of the 49 mm diameter experimental apparatus.

Models were created using the ”Free and Porous Media Flow” module, with an added second order Forchheimer term, as well as the “Turbulent Flow, k-ε” module with the low Reynolds number and incompressible options. A uniform inlet velocity and non-slip walls were assumed. Variation of the inlet conditions were experimentally tested by using L/D ratios from 22 to 65, and were found to have no influence on the obtained pressure gradients. The system pressure was defined by setting one point at the apparatus outlet as being at zero Pa gauge pressure. Velocity fields were used to define the boundary conditions between the two turbulent flow domains and the porous media domain.

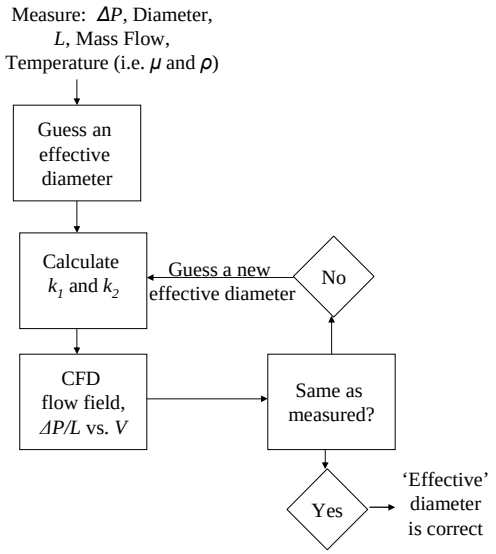

Figure 3. The FEM CFD procedure applied to the 101 mm experimental results to determine the Forchheimer parameters k_1 and k_2 [11].

The geometry used was a representation of the apparatus shown in Figure 2, using measurements with a precision of 0.1 mm. Boundary meshes (5 layers) were inserted along the outer walls where high velocity gradients were anticipated. “Normal” fluid mechanical controlled triangular mesh was used elsewhere.

Tighter meshes were tested and found to result in increased computational time and to have negligible influence on the reported results.

The pressure gradient was determined in the z-axis, by using the COMSOL 'probe' function, to establish the local pressure at the precise locations of the side wall pressure taps, see Figure 2.

5. Results

The obtained experimental pressure gradients for the 101 mm diameter filters, with long (3 m) and short inlet (1 m) lengths, are presented in Figure 4. The results for the 49 mm diameter filters are similar in appearance and have been published elsewhere [11].

The summary of the obtained Forchheimer coefficients for the 49 mm and 101 mm diameter filter elements are given in Table 1. Excellent agreement is shown between the values directly calculated from Equation (1), i.e. from the 49 mm results and those obtained by using the procedure shown previously in Figure 3, and the 101 mm filters.

A sample calculation at 0.5 m/s inlet velocity has been performed using both the FEM models for the 101 mm and 49 mm diameter filter elements. The effect of the expansion of the flow on the velocity field for the 101 mm filter element is clearly indicated in Figure 5 (a). The resulting decrease in velocity reduced the pressure gradient for the 101 mm filter element to 501 kPa/m, when compared with the 49 mm filter element with 1612 kPa/m, both at an inlet velocity of 0.5 m/s.

Table 1: Empirically Calculated (49 mm) and Numerically Derived (101 mm) Forchheimer Coefficients for Equation (1) [11].

Filter Type (PPI)	Actual Filter Diameter (m)	FEM Effective Flow Field Diameter (m)	Eq. 1 Forchheimer k_1 (m^2)	Eq. 1 Forchheimer k_2 (m)	Inlet Length (m)
30	48.7	N/A	5.08E-08	5.46E-04	1.0
30	101	65.5	5.57E-08	5.25E-04	1.0
40	101	66.0	3.10E-08	3.38E-04	1.0
50	49.2	N/A	1.57E-08	1.66E-04	1.0
50	101	66.1	1.71E-08	1.69E-04	1.0
50	101	66.1	1.52E-08	1.71E-04	3.0
80	49.1	N/A	6.52E-09	1.15E-04	1.0
80	101	66.5	5.44E-09	9.96E-05	1.0

In Figure 6 comparison is made between FEM calculated and measured results for all experimental velocities, showing individual errors between 0% and 7%, as well as average errors between 0.6% and 4% for each filter type.

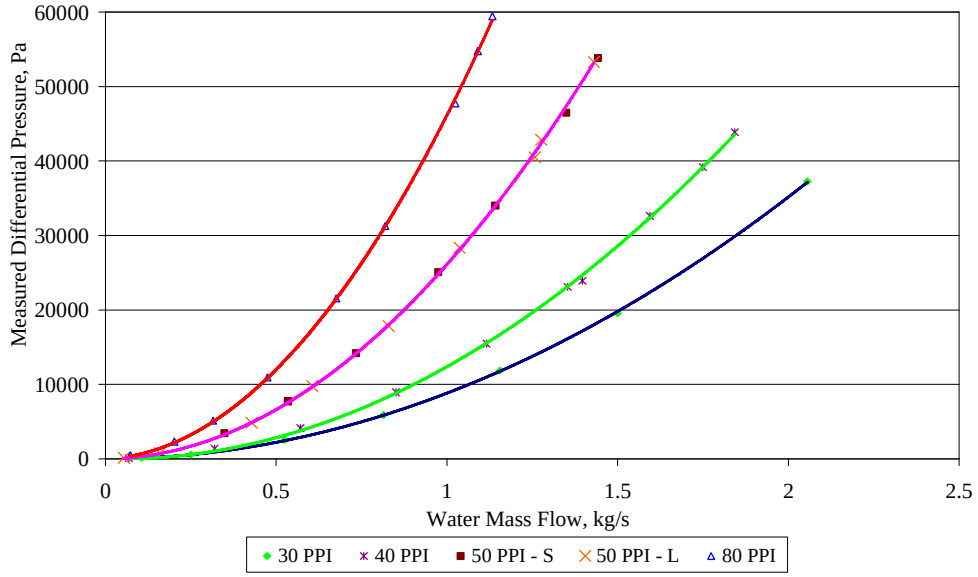

Figure 4. Experimentally measured pressure gradients for the 101 mm 'expanding flow field' design [11].

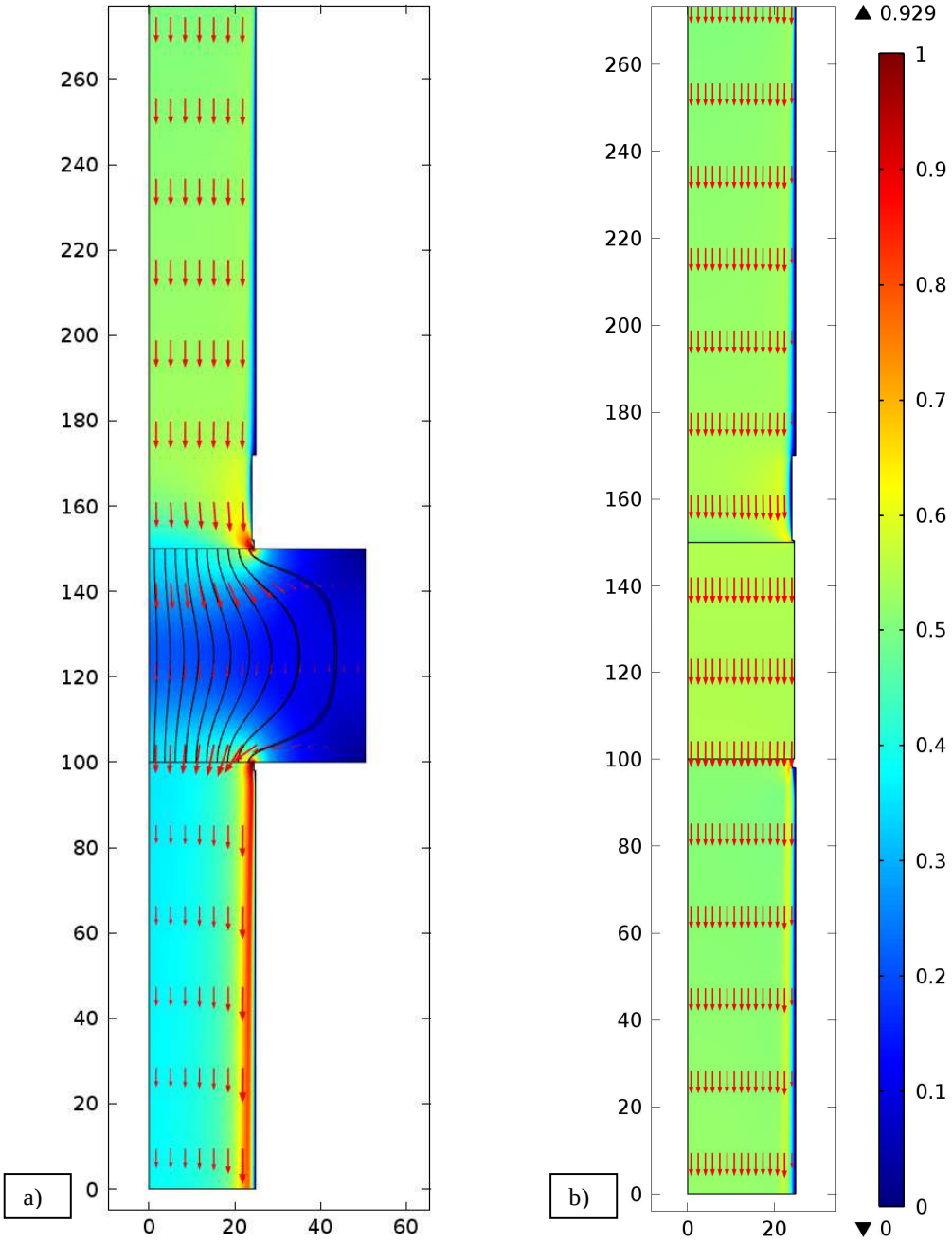

Figure 5. Comparison of calculated flow fields for 50 PPI CFF, i.e. for (a) the 101 mm 'expanding flow field' and (b) the 49 mm 'straight through' designs, both at a 0.5 m/s uniform inlet velocity and for 280 K water temperature. The results are shown with a common 0-1 m/s colour scale.

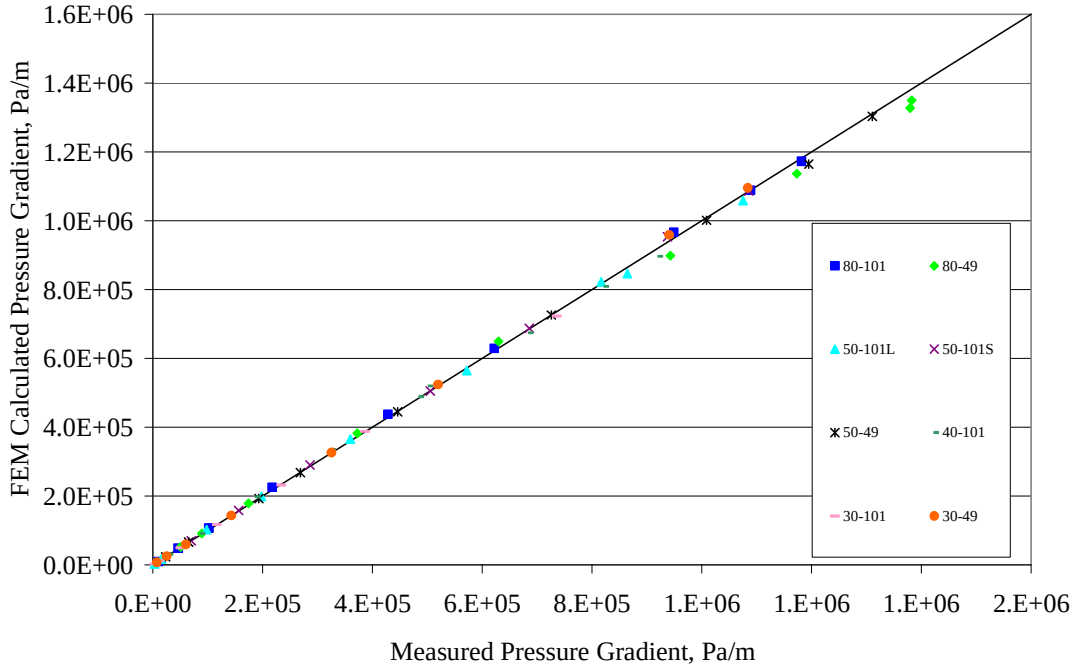

Figure 6. Comparison of FEM calculated and measured pressure gradients, indicating typical errors of <4% for each filter type. S is for a short inlet (1 m) and L is for a long inlet (3 m), as shown previously in Table 1 [11].

6. Discussion

The use of boundary meshes proved critical to achieve an acceptable agreement between model and experimental data, particularly for the 'straight through' 49 mm diameter experimental apparatus. For example, if the results shown in Figure 5 are recalculated without boundary meshes, an error of -18% is obtained for the 49 mm diameter experimental apparatus, and -8.2% for the 101 mm case. Smaller errors of ~±1% can be generated by using inappropriate slip wall boundary criteria, or by using significantly biased inlet flow conditions, rather than the assumed uniform inlet velocity.

Discrepancies between the k_1 and k_2 derived with the help of numerical methods (expanding flow field), and those directly determined experimentally (straight through), were on average within 5%, with no individual difference exceeding 17%. Deviations were such that they were compensated, i.e. a high k_1 value was compensated by a lower k_2 value, resulting in nearly identical total pressure drop for each superficial velocity.

It proved critical to avoid using the automatic second order correlation function built into Excel, as it resulted in errors being concentrated into the first order term k_1, and produced physically meaningless results, e.g. negative k_1 values. Dividing the measured pressure gradient by velocity, and using a linear regression gave improved results. The best results, i.e. those shown in Table 1, were obtained by (i) guessing k_1, (ii) subtracting the first order term from the total gradient, (iii) performing an exponential regression, and (iv) iterating until the desired exponent of 2.00000 was obtained for the second order term [11].

7. Conclusions

A high level of agreement was achieved between the experimental and the 2D axial symmetric CFD FEM results for both the 49 mm diameter 'straight through' design and the 101 mm diameter 'expanding flow field' design.

Errors in the range of ±0-7% on predicted pressure drop for individual readings were obtained in both cases.

The agreement obtained between the FEM model of the 49 mm filter apparatus, using the analytically derived Forchheimer coefficients and the experimental data, indicated that there was negligible bypassing of the filter media by the water during the experiments.

The agreement obtained between the analytical 49 mm and the 'numerical' 101 mm Forchheimer coefficients indicated the success of the iterative procedure applied in the present study to deduce the effect of the expanding flow field on the resulting pressure gradients of the 101 mm filter media.

It has been demonstrated that COMSOL can perform CFD calculations under demanding circumstances with a high level of precision, i.e. under high variation in Reynolds numbers, as well as when using both normal fluid flow and porous media.

8. References

1. D. E. Groteke, "The Reduction of Inclusions in Aluminum by Filtration," *Modern Casting*, vol. 73, (1983), 25-27.
2. H. Duval, C. Rivière, É. Laé, P. Le Brun, and J. Guillot, "Pilot-Scale Investigation of Liquid Aluminum Filtration through Ceramic Foam Filters: Comparison between Coulter Counter Measurements and Metallographic Analysis of Spent Filters," *Metallurgical and Materials Transactions B*, vol. 40, (2009), 233-246.
3. S. Instone, M. Badowski, and W. Schneider, "Development of Molten Metal Filtration Technology for Aluminium," *Light Metals*, (2005), 933-938.
4. K. Butcher and D. Rogers, "Update on the Filtration of Aluminum Alloys with Fine Pore Ceramic Foam," *Light Metals*, (1990), 797-803.
5. A. Engelbrecht, "Removal of Solid Inclusions from Molten Aluminium through Ceramic Foam Filtration," *Light Metals*, (2010), 779-784.
6. F. Frisvold, "Filtration of Aluminium: Theory, Mechanisms, and Experiments," PhD. Thesis, Norwegian University of Science and Technology, (1990).
7. C. Conti and P. Netter, "Deep Filtration of Liquid Metals: Application of a Simplified Model Based on the Limiting Trajectory Method," *Separations Technology*, vol. 2, (1992), 46-56.
8. S. Ray, B. Milligan, and N. Keegan, "Measurement of Filtration Performance, Filtration Theory and Practical Applications of Ceramic Foam Filters," *Aluminium Cast House Technology*, (2005), 1-12.
9. B. Hübschen, J. Krüger, J. Keegan, and W. Schneider, "A New Approach for the Investigation of the Fluid Flow in Ceramic Foam Filters," *Light Metals*, (2000), 809–815.
10. P. Forchheimer, "Wasserbewegung Durch Boden," *Z. Ver. Deutsch. Ing*, vol. 45, (1901), 1788.
11. M. W. Kennedy, K. Zhang, R. Fritzsch, S. Akhtar, J. A. Bakken, and R. E. Aune, "Characterization of Ceramic Foam Filters Used for Liquid Metal Filtration," *To be submitted to Metallurgical Transactions B*, (2012), 1-46.
12. L. F. Moody, "Friction Factors for Pipe Flow," *Trans. Asme*, vol. 66, (1944), 671-684.

9. Acknowledgements

The present research was carried out as part of the Norwegian Research Council (NRC) funded BIP Project (No. 179947/I40) RIRA (Remelting and Inclusion Refining of Aluminium). The project partners are as follows: Hydro Aluminium AS, SAPA Heat Transfer AB, Alcoa Norway ANS, Norwegian University of Science and Technology (NTNU) and SINTEF Materials and Chemistry. Funding by the industrial partners and NRC is gratefully acknowledged.

The authors also wish to express their gratitude to Egil Torsetnes at NTNU, Trondheim, Norway, for helping with the design and construction of the experimental apparatus. Sincere gratitude is also due to Kurt Sandaunet at SINTEF, Trondheim, Norway, for his support and help, as well as for the use of the SINTEF laboratory. The assistance of Robert Fritzsch in the SEM and optical analysis of the CFFs is greatly appreciated.